Mean-Field Theory of Polymer Interfaces in the Presence of Block Copolymers

Kenneth R. Shull*,† and Edward J. Kramer

Department of Materials Science and Engineering, Cornell University, Ithaca, New York 14853

Received December 18, 1989; Revised Manuscript Received April 13, 1990

ABSTRACT: A mean-field theory is presented that describes the effects of an A/B diblock copolymer on the properties of an interface between immiscible A and B homopolymers. A complete set of self-consistent-field equations is solved numerically in order to determine the profiles of the different polymeric components and the interfacial tension. These quantities are completely determined by the specification of the homopolymer and copolymer degrees of polymerization, a Flory–Huggins χ parameter describing the thermodynamic interactions between A and B segments, the statistical segment length, and the copolymer chemical potential. At reasonable values of this chemical potential, the interfacial tension vanishes, and the volume fraction of copolymer near the interface is close to 1. The effects of the copolymer on the interfacial properties in this strong segregation regime are governed by the extension of the copolymer blocks away from the interface and are therefore determined primarily by the degree of polymerization of the longer copolymer block. The region of molecular mixing is significantly broadened by the penetration of the copolymer chains into the homopolymer phases. There is a much smaller increase in the width of the region over which A and B segments mix, due to the constraint that the junction between the copolymer blocks must lie within this narrow region. We also find that there is a positive contribution to the interfacial tension, which may give rise to an attractive interaction between segregated polymer layers in high molecular weight polymer matrices.

Introduction

Most polymer pairs are immiscible and will form phase-separated systems when mixed together. Interfaces between polymer phases are quite fragile so that blends of immiscible homopolymers are generally of little value. The formation of useful, well-defined composite polymeric structures from preexisting homopolymers requires that the interfacial properties be carefully controlled. One way of achieving this control is by the addition of an appropriate diblock copolymer, chosen such that each block has a preferential affinity for a different homopolymer phase. Such a block copolymer will segregate preferentially to the interface between polymer phases, thereby lowering the interfacial tension. The molecular structure will also be significantly altered at the interface, a fact that can result in greatly enhanced adhesion between the two phases. Decreases in the interfacial tension in the presence of block copolymer have been observed experimentally,[1,2] as have increases in the adhesion between polymeric phases.[3,4]

We consider cases where the block copolymer at the interface is in equilibrium with the block copolymer in the bulk phases; i.e., μ_c, the block copolymer chemical potential, is spatially uniform. In practical systems this chemical potential is limited by the formation of block copolymer micelles in the bulk phases or by the formation of a separate, copolymer-rich phase. Determination of μ_c from first principles is a difficult problem, which is outside the scope of this paper. The importance of micelle formation as it pertains to the determination of μ_c is discussed in an accompanying publication,[5] as are the difficulties in reaching a true equilibrium state in real polymer systems. In the present paper we use μ_c as an independent variable and assume local equilibrium between the interface and the bulk phases.

The basic factors that give rise to the decreased interfacial tension at high values of μ_c can be qualitatively understood in terms of simple scaling arguments as outlined in a recent paper by Leibler.[6] A more sophisticated approach is necessary in order to obtain quantitative predictions and to understand the behavior at lower copolymer chemical potentials. In addition, the scaling theory does not describe the changes in molecular structure that lead to the increased adhesion. Helfand and coworkers have developed a complete mean-field theory of polymer interfaces that takes into account thermodynamic effects and polymer chain connectivity in a quantitative fashion. The theory was used to describe the interface between homopolymer melts in the absence of block copolymer[7–10] and to describe block copolymer melts that undergo microphase separation.[10–15] Hong and Noolandi developed a similar theory of polymer interfaces in the presence of a small-molecule solvent.[16–20] Hong and Noolandi considered the effects of a diblock copolymer at a homopolymer interface for the case where the polymer is diluted with solvent.[18–20] Here we develop and apply the theory for the case where no solvent is present.

Theory

We consider a three-component system of A homopolymer, B homopolymer, and an A–B diblock copolymer. The volume fraction of copolymer is ϕ_c, of which ϕ_{ca} corresponds to the A block and ϕ_{cb} corresponds to the B block. The volume fractions of A and B homopolymers are ϕ_{ha} and ϕ_{hb}, respectively. The total volume fractions of A and B segments, ϕ_a and ϕ_b, are given by $\phi_a = \phi_{ca} + \phi_{ha}$ and $\phi_b = \phi_{cb} + \phi_{hb}$. The segment concentration is ρ_0, and the degree of polymerization of component k is N_k. The free energy density, f, of a uniform system can be written in the usual Flory–Huggins form, in terms of the segment–segment interaction parameter χ_{ab}

$$\frac{f}{k_B T \rho_0} = \chi_{ab}\phi_a\phi_b + \sum_k \frac{\phi_k \ln \phi_k}{N_k} \tag{1}$$

where the reference state is a hypothetical unmixed state for which $\chi_{ab} = 0$. We use k as a subscript when the copolymer is to be considered as a single component, so that possible values for k are ha, hb, and c. When each

† Current address: IBM Almaden Research Center, 650 Harry Road, San Jose, CA 95120.

0024-9297/90/2223-4769$02.50/0

block is to be considered as a separate component, we use kc as a subscript, such that ha, hb, ca, and cb are the possible values for kc. The chemical potential, μ_k, of a molecule of component k is given by[21]

$$\frac{\mu_k}{N_k} = \frac{\partial(f/\rho_0)}{\partial\phi_k} + f/\rho_0 - \sum_k \phi_k \frac{\partial(f/\rho_0)}{\partial\phi_k} \tag{2}$$

where the derivatives with respect to a particular ϕ_k are to be taken with $\phi_{j\neq k}$ held constant. Equations 1 and 2 apply even for a composition-dependent χ_{ab}, provided that eq 1 is used as the defining relation for χ_{ab} and that there is no volume change upon mixing. Unfortunately, detailed thermodynamic information is not available for most polymer blends. We assume that χ_{ab} is independent of concentration, in which case the chemical potentials are given by

$$\frac{\mu_{ha}}{N_{ha}k_BT} = \frac{\ln \phi_{ha} + 1}{N_{ha}} - K_\phi + \chi_{ab}\phi_b^2 \tag{3}$$

$$\frac{\mu_{hb}}{N_{hb}k_BT} = \frac{\ln \phi_{hb} + 1}{N_{hb}} - K_\phi + \chi_{ab}\phi_a^2 \tag{4}$$

$$\frac{\mu_c}{N_ck_BT} = \frac{\ln \phi_c + 1}{N_c} - K_\phi + \frac{\chi_{ab}}{N_c}\{N_{ca}\phi_b^2 + N_{cb}\phi_a^2\} \tag{5}$$

with $K_\phi = \phi_{ha}/N_{ha} + \phi_{hb}/N_{hb} + \phi_c/N_c$. Later it will become necessary to distinguish between contributions to the copolymer chemical potential that arise from each separate block. The first two terms on the right-hand side of eq 5 arise from the entropy of mixing of the entire molecule with the surrounding chains and are common to both blocks. The term involving χ_{ab} arises from interactions between each separate block and the overall surroundings, and this term can be split between the two blocks. One then arrives at the following expressions for μ_{ca} and μ_{cb}, the effective chemical potentials of A and B copolymer blocks, respectively, defined such that $\mu_c = \mu_{ca} + \mu_{cb}$:

$$\frac{\mu_{ca}}{N_{ca}k_BT} = \frac{\ln \phi_c + 1}{N_c} - K_\phi + \chi_{ab}\phi_b^2 \tag{6}$$

$$\frac{\mu_{cb}}{N_{cb}k_BT} = \frac{\ln \phi_c + 1}{N_c} - K_\phi + \chi_{ab}\phi_a^2 \tag{7}$$

An unfavorable enthalpic interaction between A and B segments gives rise to a phase separation into A-rich and B-rich phases. The volume fractions of the three different components in each of the two separate phases completely define the system away from the interface. Three constraints on these six quantities arise by equating the chemical potentials of the components in each phase. An additional two constraints arise by requiring that the volume fractions in each phase sum to 1. The compositions of the bulk phases are therefore completely determined by the specification of any single volume fraction or chemical potential. It is generally most convenient to use μ_c as the independent variable, since μ_c is often fixed by the formation of copolymer micelles in one or both of the bulk phases. In addition, we will often consider highly incompatible systems where the bulk phases are nearly pure homopolymer such that μ_{ha} and μ_{hb} are very close to zero.

The interfacial tension between the two phases is determined primarily by constraints imposed by the polymer chain connectivity. This situation is in contrast to the situation for small-molecule systems, where the interfacial tension arises from nonlocal terms in the expression for the free energy.[22] Polymer chains in a homogeneous melt obey Gaussian statistics so that the chain dimensions can be completely characterized in terms of a single parameter. The most convenient parameter is the statistical segment length, a, defined such that a^2 is the ratio of $\langle R^2\rangle$, the mean-squared end-to-end distance of a polymer chain, to the degree of polymerization of the polymer chain:

$$a^2 = \langle R^2\rangle/N \tag{8}$$

Equation 8 has an analogy in classical diffusion, where the tracer diffusion coefficient is defined as the ratio of $\langle r^2\rangle$, the mean-squared displacement of a particle, to the time τ over which the displacement takes place:

$$D = \langle r^2\rangle/6\tau \tag{9}$$

Comparison of eq 8 and 9 indicates that one can formally describe the polymer chain as a diffusing particle with an effective diffusion coefficient of $a^2/6$. The effective time is a normalized curvilinear distance as measured from one end of the chain and can take on values from 0 to N_k. As initially described by Edwards,[23] this analogy can be exploited in order to develop a theory of inhomogeneous polymer systems. The central quantities are distribution functions $q_k(x,n)$, which represent the probability that a given k chain has reached a position x after "time" n. In the presence of a weakly varying perturbing field, $w_k(x)$, which acts on the polymer segments, $q_k(x,n)$ must satisfy the modified diffusion equation[23]

$$\frac{\partial q_k(x,n)}{\partial n} = \frac{a^2}{6}\frac{\partial^2 q_k(x,n)}{\partial x^2} - \frac{w_k(x)}{k_BT}q_k(x,n) \tag{10}$$

with the following initial condition:

$$q_k(x,0) = 1 \tag{11}$$

The function $w_k(x)$ is a position-dependent mean field, which is related to the local composition. It is convenient to replace n with $t = n/N_k$, a continuous variable, which runs from 0 to 1, such that eq 10 becomes

$$\frac{1}{N_k}\frac{\partial q_k(x,t)}{\partial t} = \frac{a^2}{6}\frac{\partial^2 q_k(x,t)}{\partial x^2} - \frac{w_k(x)}{k_BT}q_k(x,t) \tag{12}$$

A point along a given polymer chain is characterized by the diffusion paths from the two distinct chain ends, and the probability of finding such a point will be the product of two distribution functions, $q_k(x,t)$ and $q_k(x,1-t)$. The polymer volume fraction is given by the integration over all possible junction points

$$\phi_k(x) = A_k\int_0^1 q_k(x,t)\, q_k(x,1-t)\, dt \tag{13}$$

where A_k is a normalization factor, which must be consistent with the values of ϕ_k in the bulk phases.

Equations 12 and 13 apply directly to the homopolymers, with k = ha for the A homopolymer and k = hb for the B homopolymer. The block copolymer contains different segment types, however, and the approach outlined above is applicable only if a t-dependent mean-field is used. Following Hong and Noolandi,[18] we use an alternate approach, where four different distribution functions are used to define the block copolymer. Each distribution function corresponds to a different portion of the block copolymer, as shown in Figure 1. The A block is characterized by q_{ca} corresponding to a segment originating from the free end and q_{ab} corresponding to a segment originating from the junction with the B block. Similarly, the B block is characterized by q_{cb} and q_{ba},

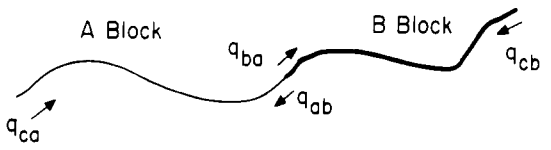

Figure 1. Schematic diagram of a copolymer chain showing the starting points for the diffusion paths represented by the probability distribution functions q_{ca}, q_{cb}, q_{ab}, and q_{ba}.

corresponding to segments originating from the free end and the junction, respectively.

The diffusion equations for q_{ca} and q_{ab} are identical with eq 12, with $N_k = N_{ca}$ and $w_k = w_{ca}$. The diffusion equations for q_{cb} and q_{ba} are also identical with eq 12, with $N_k = N_{cb}$ and $w_k = w_{cb}$. The connectivity of the two blocks appears in the initial conditions for q_{ab} and q_{ba}; i.e., $q_{ab}(x,0) = q_{cb}(x,1)$ and $q_{ba}(x,0) = q_{ca}(x,1)$. The initial conditions for q_{ca} and q_{cb} are $q_{ca}(x,0) = q_{cb}(x,0) = 1$ as given by eq 11. The A block volume fraction is given by

$$\phi_{ca}(x) = A_{ca} \int_0^1 q_{ca}(x,t)\, q_{ab}(x,1-t)\, dt \tag{14}$$

Similarly, the B block volume fraction is given by

$$\phi_{cb}(x) = A_{cb} \int_0^1 q_{cb}(x,t)\, q_{ba}(x,1-t)\, dt \tag{15}$$

The mean fields are specified only to within a constant factor c_k and are related to the chemical potentials. Hong and Noolandi obtained expressions for the mean fields by using the Flory–Huggins form for the local free energy density across the interface.[16] We neglect nonlocal contributions to the segment–segment interactions, in which case the Hong and Noolandi result reduces to

$$w_{kc}(x) = \frac{\mu_{kc}(x)}{N_{kc}} - \frac{k_B T \ln \phi_k(x)}{N_k} - \Delta w(x) - c_k \tag{16}$$

with $\mu_{kc}(x)$ as given by eqs 3, 4, 6, and 7. The quantity $\Delta w(x)$ vanishes in the bulk phases and is associated with the requirement that the segment density remain constant across the interface. The interfacial tension, γ, is given by the integral of $\Delta w(x)$:[12,16]

$$\gamma = \rho_0 \int_{-\infty}^{+\infty} \Delta w(x)\, dx \tag{17}$$

The following relationship between A_{kc} and c_k is defined by the requirement that the mean-field equations give the correct volume fractions in the bulk phases, where $\Delta w = 0$:

$$A_{kc} = \frac{N_{kc}}{N_k} \exp\left(-\frac{\mu_k - c_k N_k}{k_B T}\right) \tag{18}$$

We chose $c_k = k_B T / N_k$ so that there are only two distinct mean fields, w_a and w_b:

$$w_a(x) = w_{ha}(x) = w_{ca}(x) = k_B T(\chi_{ab}\phi_b^2(x) - K_\phi(x)) - \Delta w(x) \tag{19}$$

$$w_b(x) = w_{hb}(x) = w_{cb}(x) = k_B T(\chi_{ab}\phi_a^2(x) - K_\phi(x)) - \Delta w(x) \tag{20}$$

From eq 18 one has $A_{ha} = \exp(\mu_{ha}/k_B T - 1)$, $A_{hb} = \exp(\mu_{hb}/k_B T - 1)$, $A_{ca} = (N_{ca}/N_c)\exp(\mu_c/k_B T - 1)$, and $A_{cb} = (N_{cb}/N_c)\exp(\mu_c/k_B T - 1)$.

The presence of a small-molecule solvent simplifies the expression for $\Delta w(x)$, since there are no constraints on the positions of individual solvent molecules as there are for individual polymer segments. As a result one obtains $\Delta w = \Delta\mu_s$, where $\Delta\mu_s$ is the excess solvent chemical potential, i.e. $\mu_s(x) - \mu_s^{bulk}$ as given by the combination of eqs 1 and 2, and $\rho_0 \Delta w(x)$ is the negative of the osmotic pressure. Hong and Noolandi have used this result in order to obtain explicit equations for the mean fields.[16-19] As discussed below, it is also easier to obtain a self-consistent solution to the mean-field equations for the case where a solvent is present.

For the case where no solvent is present the expression for Δw can be written in terms of a parameter ζ, which is inversely proportional to the bulk compressibility, as described in the series of papers by Helfand and his collaborators:[7-15]

$$\Delta w = \zeta(1 - \sum_k \phi_k) \tag{21}$$

For infinite molecular weight homopolymers in the absence of block copolymer there are only two distribution functions, q_{ha} and q_{hb}, and these are no longer functions of t. An analytic solution to this "steady-state" problem was obtained by Helfand and Tagami in terms of a series in χ_{ab}/ζ.[8] For $\chi_{ab}/\zeta = 0$, corresponding to the assumption of incompressibility, they obtain the following:

$$\phi_{ha}(x) = (1/2) + (1/2)\tanh\{(6\chi_{ab})^{1/2}(x/a)\} \tag{22}$$

$$\phi_{hb}(x) = 1 - \phi_{ha}(x) \tag{23}$$

Here $x = 0$ at the center of the interface; i.e., $\phi_{ha}(0) = \phi_{ha}(0) = 0.5$. The interfacial tension obtained for this infinite molecular weight limit is γ_0^∞, given by

$$\gamma_0^\infty = a\rho_0 k_B T(\chi_{ab}/6)^{1/2} \tag{24}$$

It is convenient to define the quantity d, which is a measure of the width over which A and B segments mix:

$$d = (\partial\phi_a/\partial x)_{x=0}^{-1} \tag{25}$$

We define d_0 as the value of d in the absence of copolymer, in which case $\phi_a = \phi_{ha}$. Substitution of the hyperbolic tangent profile of eq 22 into eq 25 gives the following for d_0^∞, the infinite molecular weight limit of d_0:

$$d_0^\infty = 2a/(6\chi_{ab})^{1/2} \tag{26}$$

Numerical methods must be used in order to obtain solutions to the mean-field equations for more complex situations, such as when copolymer is present at the interface. Solutions to the mean-field equations for polymer melts are difficult to obtain by numerical methods because of the high values of ζ for these melts. A lower effective ζ can be defined when there is a significant amount of solvent present,[8] thus simplifying the solution considerably. We have developed a method for solving the mean-field equations for high values of ζ so that the inclusion of a solvent is no longer necessary. Our procedure is described in detail in the Appendix.

Results

In this section we present results from calculations that illustrate the dependencies of the interfacial properties on the molecular parameters. We refer to block copolymers by the degrees of polymerization of the A and B blocks. A 200–100 copolymer, for example, has $N_{ca} = 200$ and $N_{cb} = 100$. In all cases we use homopolymer degrees of polymerization that are equal to one another, such that $N_{ha} = N_{hb} = N_h$.

Profiles for a 200–200 copolymer at a homopolymer interface are shown in Figure 2, where we have used $N_h = 1000$, $\mu_c = 4k_B T$, and $\chi_{ab} = 0.1$. Distances are scaled to the statistical segment length a. The copolymer and homopolymer volume fractions are shown in Figure 2a,

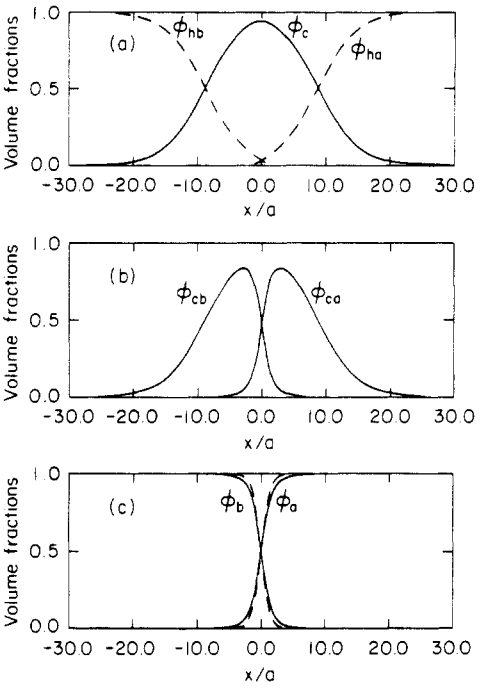

Figure 2. Interfacial profiles for $N_{ca} = N_{cb} = 200$, $N_{ha} = N_{hb} = 1000$, $\chi_{ab} = 0.1$, and $\mu_c = 4k_BT$: (a) homopolymer volume fractions (- - -) and the copolymer volume fraction (—), (b) volume fractions of the individual copolymer blocks, (c) overall volume fractions of A and B segments in the presence of copolymer (—), and in the absence of copolymer (- - -).

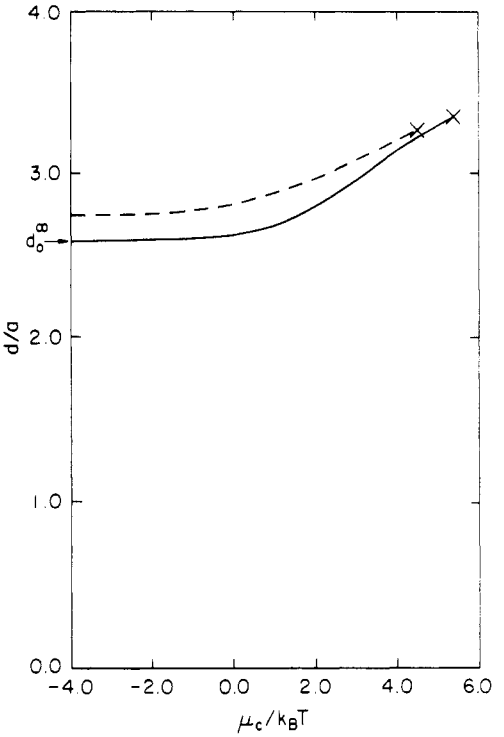

Figure 3. Width of segmental profile as a function of μ_c for $N_{ca} = N_{cb} = 200$, and $\chi_{ab} = 0.1$: $N_{ha} = N_{hb} = 1000$ (—), $N_{ha} = N_{hb} = 200$ (- - -).

whereas the volume fractions of the individual copolymer blocks are shown in Figure 2b. The distributions of A and B segments, regardless of their placement on homopolymer or copolymer chains, are shown in Figure 2c. The segment profiles of Figure 2c are somewhat broadened in comparison to the profiles obtained in the absence of copolymer. The value of d/a corresponding to the profiles of Figure 2c is 3.20, whereas d_0/a is equal to 2.58. This broadening of the segment profile arises from the constraint that the junction between the copolymer blocks must lie within the narrow interfacial region of width d. The entropic penalty associated with this constraint is lower for higher values of d, and there is therefore an extra driving force for the broadening of the segment profiles in the presence of block copolymers.

Figure 3 shows d as a function of μ_c for a 200–200 copolymer with $\chi_{ab} = 0.1$. Separate curves are included for $N_h = 200$ (dashed line) and $N_h = 1000$ (solid line). The value of d_0 for $N_h = 1000$ is very close to d_0^∞ as given by eq 26, whereas d_0 for $N_h = 200$ is increased from this infinite molecular weight value by 6%. The maximum value of d, corresponding to the value of μ_c for which γ vanishes, is increased from d_0 by 19% for $N_h = 200$ and by 30% for $N_h = 1000$. These increases in the widths of the segmental profiles are not expected to contribute significantly to the mechanical properties of the interface. As shown in parts a and b of Figure 2, the block copolymer mixes with the homopolymer over a region having a width of several times d_0. In contrast to the hypothesis of Brown,[3] it is this penetration of the block copolymer into the homopolymer phases, not the increase in the segmental mixing, that must be primarily responsible for the enhanced adhesion between the different phases at equilibrium.

We use two related quantities to describe the total copolymer excess at the interface. The first quantity is z_i^*, corresponding to the area under the ϕ_c profile of Figure 2a and defined as follows:

$$z_i^* = \int_{-\infty}^{+\infty} (\phi_c(x) - \phi_c^{bulk})\, dx \tag{27}$$

For positive values of x, ϕ_c^{bulk} is equal to ϕ_c^A, the copolymer volume fraction in the bulk A-rich phase. For negative values of x, ϕ_c^{bulk} is equal to ϕ_c^B, the copolymer fraction in the bulk B-rich phase. The interfacial copolymer excess in chains per unit area, ν_i, is obtained from z_i^* by dividing by the copolymer molecular volume:

$$\nu_i = z_i^* \rho_0 / N_c \tag{28}$$

The Gibbs adsorption equation defines a relationship between the interfacial tension, the chemical potentials of the different molecular components, and the interfacial excesses of these components. Terms involving the chemical potentials of the homopolymers can be ignored when the solubility of the copolymer in the bulk phases is very small, so that one obtains

$$\nu_i = -d\gamma/d\mu_c \tag{29}$$

which can be integrated to give

$$\gamma = \gamma_0 - \int_{-\infty}^{\mu_c} \nu_i(\mu_c')\, d\mu_c' \tag{30}$$

where γ_0 is the interfacial tension in the absence of block copolymer.

The copolymer chemical potential is a better parameter for describing the state of the system than ϕ_c^A or ϕ_c^B. Micelles form at a critical copolymer chemical potential, μ_{cmc}, which may correspond to very low values of ϕ_c^A and ϕ_c^B. When the solubility of block copolymer is low, eq 5 can be rewritten to give the following expression for ϕ_c^A:

$$\phi_c^A = \exp\left(\frac{\mu_c}{k_BT} + \frac{N_c}{N_h} - 1 - \chi_{ab}N_{cb}\right) \tag{31}$$

A similar expression for ϕ_c^B is obtained by substituting N_{ca} for N_{cb} in eq 31, and the argument that follows is applicable to the B-rich phase when the appropriate

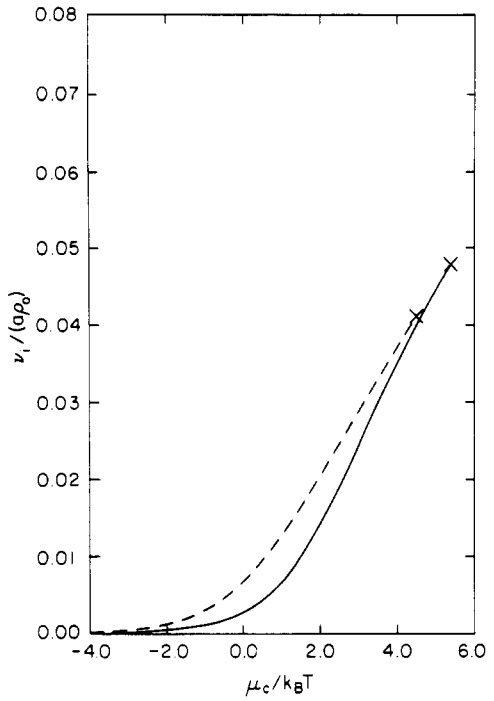

Figure 4. Normalized interfacial density of copolymer chains as a function of μ_c for $N_{ca} = N_{cb} = 200$ and $\chi_{ab} = 0.1$ with $N_{ha} = N_{hb} = 1000$ (—) and with $N_{ha} = N_{hb} = 200$ (- - -).

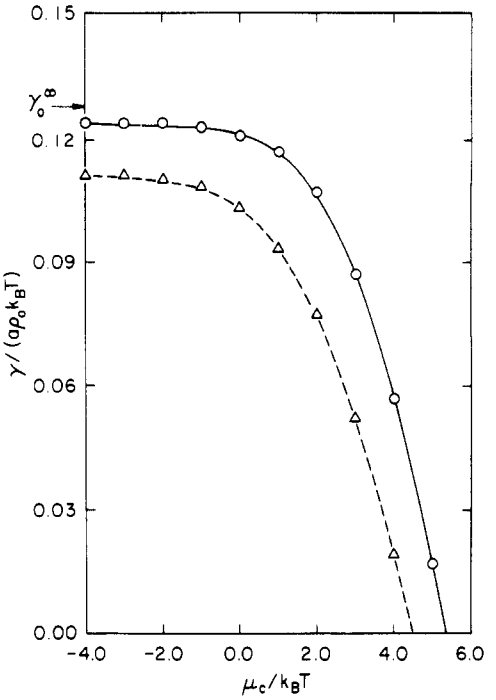

Figure 5. Normalized interfacial tension as a function of μ_c for $N_{ca} = N_{cb} = 200$ and $\chi_{ab} = 0.1$: $N_{ha} = N_{hb} = 1000$ (○—), $N_{ha} = N_{hb} = 200$ (△- - -). The symbols represent values calculated from theory by integration of Δw, and the lines represent values calculated by integration of the data shown in Figure 4.

substitutions are made. When $\chi_{ab}N_{cb}$ is significantly greater than μ_c, the copolymer concentration in the bulk A-rich phase as given by eq 31 will be very low. If the copolymer concentration in the bulk A-rich phase is greater than $\phi_c^A(\mu_c=\mu_{cmc})$ as given by eq 31, micelles will be present and eq 31 gives the volume fraction of free block copolymer chains.[24] However, the mean-field relationship between ϕ_c and μ_c may no longer be appropriate for very low copolymer concentrations where the copolymer chains exist as separated polymer coils. Equation 31 will still be a good approximation for the volume fraction of free copolymer chains, provided that the individual coils retain their ideal Gaussian configurations so that the local copolymer concentration within a given coil is quite low. Nevertheless, it is better to use μ_c as the independent variable so that errors associated with the extrapolation of the mean-field equations to the dilute regime are eliminated. Mean-field theory is expected to give an accurate description of the interfacial region where the copolymer volume fraction is generally quite high, provided that the proper copolymer chemical potential is used.

The dependencies of ν_i and γ on the copolymer chemical potential for the system corresponding to the profiles in Figure 2 are plotted in Figures 4 and 5, respectively. Values for $N_h = 200$ are also included. As a check on the consistency of the solution, the values of the surface tension as obtained from the copolymer excess and eq 30 are plotted as the solid lines in Figure 5. The symbols in Figure 5 represent the values of the interfacial tension as calculated from the integration of Δw according to eq 17 and are in excellent agreement with the values derived from the copolymer excess. We obtain $\gamma_0 = 0.125\rho_0 a k_B T$ for $N_h = 1000$ and $\chi_{ab} = 0.1$, which is very close to the value of $0.129\rho_0 a k_B T$ given by eq 24 for the infinite molecular weight limit. When N_h is decreased to 200, we obtain $\gamma_0 = 0.111\rho_0 a k_B T$. In addition, the μ_c dependence of ν_i, and therefore of the decrease in γ, is different for the two homopolymer molecular weights.

Very often one is interested in the case where μ_c is relatively high such that γ is significantly reduced from γ_0 and the copolymer volume fraction in the interfacial region is appreciable. Here we examine the importance of χ_{ab}, N_{ca}, and N_{cb} on the tendency for a block copolymer to segregate to the interface and reduce the interfacial tension. We consider a series of copolymers where in all cases $\mu_c = 4k_BT$ and $N_h = 1000$. The values given for ϕ_c^A and ϕ_c^B are approximations based on the representation of the dilute copolymer solutions by the mean-field picture as described above.

Table I
Calculated Interfacial Parameters for Different Values of χ_{ab}, with $N_h = 1000$, $N_{ca} = N_{cb} = 200$, and $\mu_c = 4k_BT$

χ_{ab}	ϕ_c^{bulk}	$\nu_i/a\rho_0$	$\gamma/a\rho_0k_BT$	$\gamma_0/a\rho_0k_BT$	$\Delta\gamma/a\rho_0k_BT$
0.05	1.4×10^{-3}	0.040	0.002	0.086	0.084
0.06	1.9×10^{-4}	0.039	0.016	0.095	0.079
0.07	2.5×10^{-5}	0.038	0.028	0.103	0.075
0.08	3.4×10^{-6}	0.037	0.039	0.110	0.071
0.09	4.6×10^{-7}	0.036	0.049	0.117	0.069
0.10	6.2×10^{-8}	0.035	0.057	0.124	0.067

The χ_{ab} dependencies of the interfacial properties for a 200–200 copolymer are illustrated by the data in Table I. The interfacial copolymer excess and the decrease in the interfacial tension from γ_0 are plotted in Figure 6. The interfacial copolymer excess is only weakly dependent on χ_{ab}, whereas the decrease in the interfacial tension from γ_0 shows a greater dependence on χ_{ab}. The copolymer distributions and A/B segment profiles for $\chi_{ab} = 0.05$ and $\chi_{ab} = 0.10$ are compared in Figure 7. The A/B segment profile is narrower for higher values of χ_{ab}. As discussed in the next section, the effects of an increasing χ_{ab} can be understood in terms of the localization of the copolymer joints to this narrower interfacial region.

The effects of varying the copolymer molecular weight are illustrated by the data in Table II, where we have used $\chi_{ab} = 0.1$. Data for three sets of polymers are included, where each set has N_{ca} varying from 100 to 1000. The first set is a series of symmetric copolymers with $N_{ca} = N_{cb}$. The second and third sets have N_{cb} fixed at 100 and 1000,

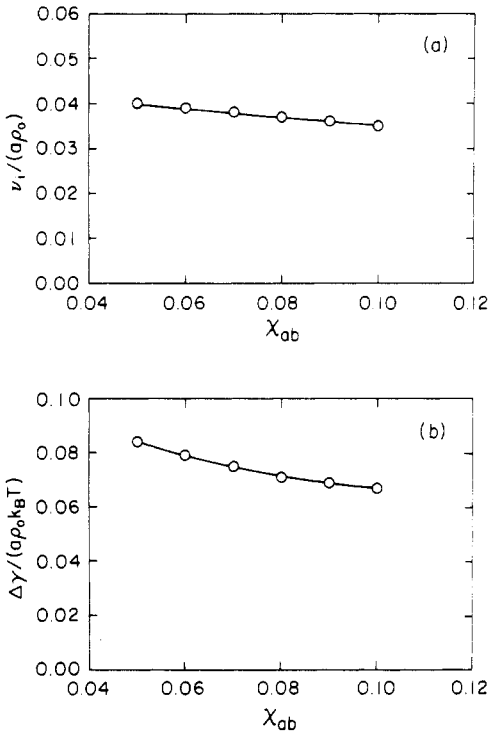

Figure 6. Interfacial parameters as a function of χ_{ab} for $N_{ca} = N_{cb} = 200$, $N_{ha} = N_{hb} = 1000$, and $\mu_c = 4k_BT$: (a) normalized interfacial density of copolymer chains, (b) normalized decrease in the interfacial tension due to the presence of the copolymer.

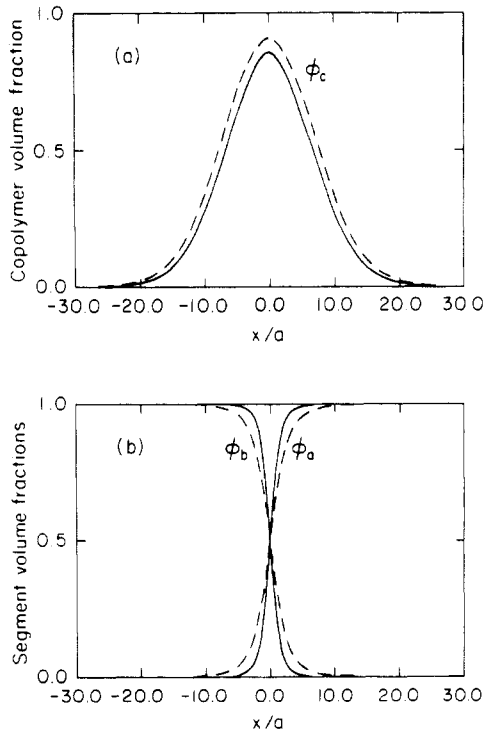

Figure 7. Interfacial profiles for $N_{ca} = N_{cb} = 200$, $N_{ha} = N_{hb} = 1000$, and $\mu_c = 4k_BT$, with $\chi_{ab} = 0.1$ (—) and with $\chi_{ab} = 0.05$ (- - -): (a) copolymer volume fraction, (b) total volume fractions of A segments and of B segments.

respectively. The interfacial copolymer excess and the interfacial tension for these three sets of copolymers are plotted in Figure 8. These interfacial parameters vary only slightly when the degree of polymerization of the shorter block is altered but vary significantly when the degree of polymerization of the longer block is altered. In addition, the curves for $N_{cb} = N_{ca}$ are quite close to the curves for $N_{cb} = 100$. Together, these data illustrate the important

Table II
Calculated Interfacial Parameters for Different Diblock Copolymers, with $N_h = 1000$, $\mu_c = 4k_BT$, $\chi_{ab} = 0.1$, and $\gamma_0/a\rho_0k_BT = 0.124$

N_{ca}–N_{cb}	ϕ_c^A	ϕ_c^B	z_i^*/a	$\nu_i/a\rho_0$	$\gamma/a\rho_0k_BT$
100–100	1.1×10^{-3}	1.1×10^{-3}	11.4	0.0568	0.010
200–200	6.2×10^{-8}	6.2×10^{-8}	14.1	0.0353	0.057
400–400	1.9×10^{-16}	1.9×10^{-16}	18.1	0.0226	0.081
600–600	5.8×10^{-25}	5.8×10^{-25}	21.3	0.0178	0.089
800–800	1.8×10^{-33}	1.8×10^{-33}	24.4	0.0152	0.092
1000–1000	5.5×10^{-42}	5.5×10^{-42}	27.3	0.0137	0.094
100–1000	2.2×10^{-42}	2.8×10^{-3}	20.1	0.0183	0.087
200–1000	2.5×10^{-42}	1.4×10^{-7}	20.9	0.0174	0.089
400–1000	3.0×10^{-42}	3.5×10^{-16}	22.6	0.0162	0.091
600–1000	3.7×10^{-42}	8.7×10^{-25}	24.3	0.0152	0.092
800–1000	4.5×10^{-42}	2.2×10^{-33}	25.8	0.0144	0.093
1000–1000	5.5×10^{-42}	5.5×10^{-42}	27.3	0.0137	0.094
100–100	1.1×10^{-3}	1.1×10^{-3}	11.4	0.0568	0.010
200–100	1.2×10^{-3}	5.6×10^{-8}	12.8	0.0427	0.041
400–100	1.5×10^{-3}	1.4×10^{-16}	15.2	0.0303	0.066
600–100	1.9×10^{-3}	3.5×10^{-25}	17.0	0.0243	0.077
800–100	2.2×10^{-3}	8.9×10^{-34}	18.6	0.0207	0.083
1000–100	2.8×10^{-3}	2.2×10^{-42}	20.1	0.0183	0.087

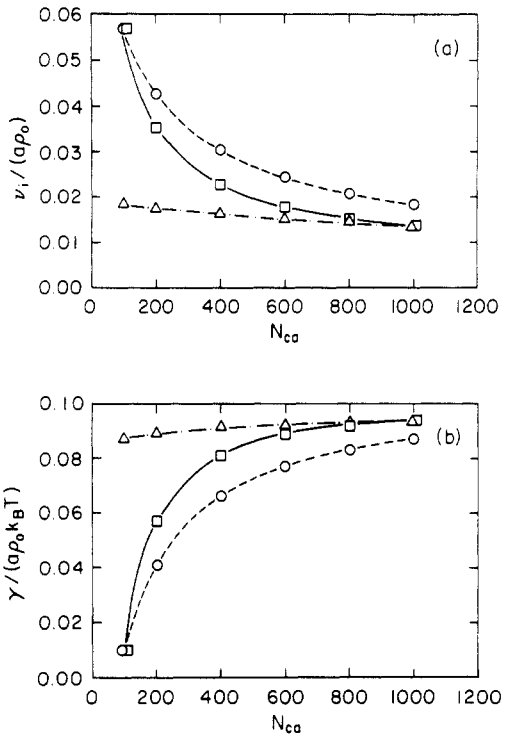

Figure 8. Interfacial parameters as a function of N_{ca} for $N_{ha} = N_{hb} = 1000$, $\mu_c = 4k_BT$, and $\chi_{ab} = 0.1$, with $N_{cb} = N_{ca}$ (□—), $N_{cb} = 100$ (○- - -), and $N_{cb} = 1000$ (△-·-): (a) normalized interfacial density of copolymer chains, (b) normalized interfacial tension.

point that the interfacial properties are dominated by the length of the longer copolymer block.

At a given value of μ_c, the ability of a block copolymer to reduce the interfacial tension is highest for smaller block copolymers and for smaller values of χ_{ab}. However, at a given value of ϕ_c^A longer copolymers with a higher χ_{ab} have a much higher interfacial activity, due to the exponential dependence of μ_c on $\chi_{ab}N_b$. In addition, larger block copolymers may be more effective at increasing the interfacial adhesion, since the extension of the copolymer into bulk phases is increased. For use in practical situations, N_c and χ_{ab} should be optimized so that the desired interfacial properties are obtained, taking into account kinetic limitations associated with the formation of micelles at very low copolymer concentration.[5]

Asymmetric polymers will favor curved interfaces,[6,25] whereas we have assumed that the interface is completely

flat. The formation of a curved interface from an initially flat interface is accompanied by an increased interfacial area and will be thermodynamically favorable only when the interfacial tension is small. Our description of a flat interface is therefore valid for cases where the interfacial tension is relatively large or when a flat interface is metastable. A description of the equilibrium structure for a near-vanishing interfacial tension requires that the effects of curvature be considered.

Discussion

In order to understand the physical effects associated with the presence of block copolymers at homopolymer interfaces, we begin with a description of homopolymer interfaces in the absence of block copolymer. An equivalent derivation of the interfacial properties for very high molecular weight homopolymers begins with the following expression for the free energy

$$F/A = \rho_0 \int_{-\infty}^{+\infty} \{f(x) + k(x)\}\, dx \tag{32}$$

where $f(x)$ is the local free energy density as given by eq 1 and $k(x)$ represents the free energy associated with concentration gradients across the interface. The functional form of $k(x)$ is[26,27]

$$\frac{k(x)}{k_B T} = \frac{a^2}{24\phi_{ha}(x)}\left\{\frac{\partial\phi_{ha}(x)}{\partial x}\right\}^2 + \frac{a^2}{24\phi_{hb}(x)}\left\{\frac{\partial\phi_{hb}(x)}{\partial x}\right\}^2 = \frac{a^2}{24\phi_{ha}(x)\,\phi_{hb}(x)}\left\{\frac{\partial\phi_{ha}(x)}{\partial x}\right\}^2 \tag{33}$$

The interfacial tension is given by subtracting the free energy of a homogeneous system from the overall free energy:

$$\gamma_0 = \rho_0 \int_{-\infty}^{+\infty} \left\{f(x) + k(x) - \frac{\mu_{ha}}{N_{ha}} - \frac{\mu_{hb}}{N_{hb}}\right\} dx \tag{34}$$

The interfacial profiles are obtained by minimizing γ_0, subject to the constraints imposed by the mean-field equations. A statement of these constraints in the infinite molecular weight, zero compressibility limit is[26]

$$f(x) - \frac{\mu_{ha}}{N_{ha}} - \frac{\mu_{hb}}{N_{hb}} = k(x) \tag{35}$$

Comparison to eq 17 for $\Delta w(x)$ indicates that $\Delta w_0(x)$, the value of $\Delta w(x)$ in the absence of copolymer, has the following explicit form, valid when the radius of gyration of the homopolymers is much greater than d_0:

$$\frac{\Delta w_0(x)}{k_B T} = \frac{2k(x)}{k_B T} = \frac{a^2}{12\phi_{ha}(x)\,\phi_{hb}(x)}\left\{\frac{\partial\phi_{ha}(x)}{\partial x}\right\}^2 \tag{36}$$

When the interfacial width d_0 is much larger than the homopolymer radius of gyration, $k(x)$ is given by[26]

$$\frac{k(x)}{k_B T} = \frac{a^2}{36\phi_{ha}(x)\,\phi_{hb}(x)}\left(\frac{\partial\phi_{ha}(x)}{\partial x}\right)^2 \tag{37}$$

For intermediate values of the ratio R_g/d_0, $k(x)$ will vary smoothly between the two forms given by eqs 33 and 37.

The infinite molecular weight limit of $\Delta w_0(x)$ is obtained by substituting the hyperbolic tangent profile of eq 22 into eq 36 for $\Delta w_0(x)$. The result for $\chi_{ab} = 0.1$ is represented by the solid line in Figure 9, along with $\Delta w_0(x)$ as obtained from the numerical calculations for $N_h = 1000$ and for $N_h = 200$. There are two origins for the decrease in Δw_0 from the infinite molecular weight limit, the first of which is the decrease in the coefficient of the squared gradient term with decreasing homopolymer molecular weight as described above. In addition, the entropic penalty associated with the confinement of smaller homopolymers to their respective half spaces causes the interfacial region to broaden so that the gradient itself is decreased. Broseta et al. obtained an expression for this contribution to the decrease in γ_0 by using the infinite molecular weight form of $k(x)$ as given by eq 33.[26]

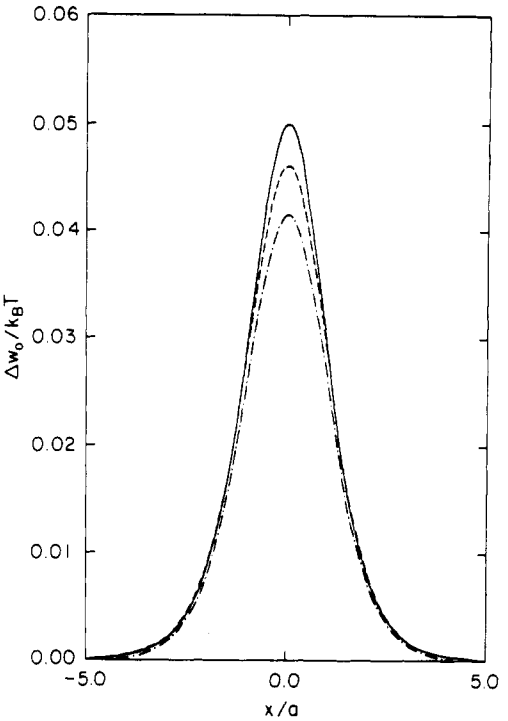

Figure 9. Excess free energy, Δw, in the absence of copolymer for $\chi_{ab} = 0.1$: $N_{ha} = N_{hb} = \infty$ (—), $N_{ha} = N_{hb} = 1000$ (- - -), $N_{ha} = N_{hb} = 200$ (- · -).

The form of $\Delta w(x)$ is much more complicated when block copolymer is present at the interface. The calculated Δw profile for a 200–200 copolymer at an interface between homopolymers with $N_h = 1000$ is shown in Figure 10, where we have used $\mu_c = 4k_BT$ and $\chi_{ab} = 0.1$. The Δw profile for these homopolymers in the absence of copolymer is shown for comparison, and the calculated interfacial profiles for these parameters are as shown in Figure 2.

It is at best very difficult to derive an accurate analytic expression for the interfacial tension in the presence of block copolymers, although it is possible to examine the contributions to the interfacial tension, which gave rise to the qualitative form of the Δw profile shown in Figure 10. Here we examine these contributions in terms of a simple model of the interfacial structure, which is similar to the model described by Leibler in ref 6. The model is valid when a highly concentrated copolymer layer exists at the interface, in which case there will actually be three distinct interfaces that contribute to the overall interfacial tension. One interface separates the A and B blocks of the copolymer and two interfaces separate these copolymer layers from their respective bulk phases. It will prove useful to assign each interface its own contribution to the overall interfacial free energy, as shown schematically in Figure 11.

The overall free energy of the interfacial region includes the stretching free energy of the copolymer chains in

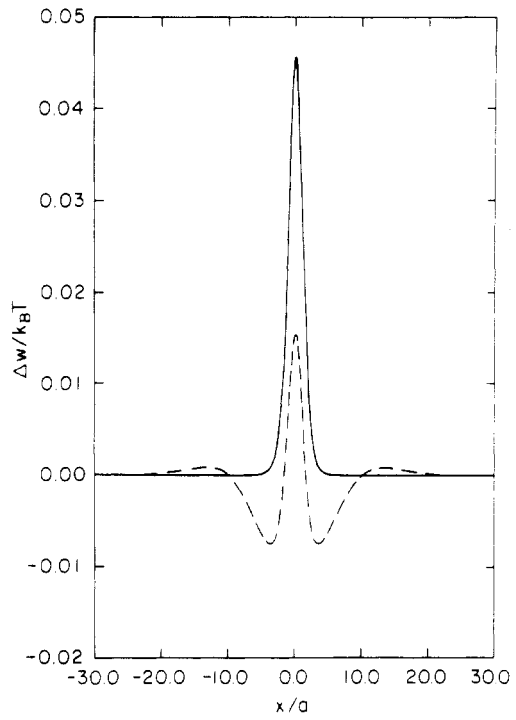

Figure 10. Excess free energy, Δw, for $\chi_{ab} = 0.1$ and $N_{ha} = N_{hb} = 1000$: in the absence of copolymer (—) and for a 200–200 copolymer with $\mu_c = 4k_BT$ (- - -).

addition to the interfacial free energies

$$\frac{F}{A_{int}} = \gamma_{ca\text{-}cb} + \gamma_{ca\text{-}ha} + \gamma_{cb\text{-}hb} + \frac{3Qk_BT}{2A_{int}}\left\{\frac{\langle R_a^2\rangle}{N_{ca}a^2} + \frac{\langle R_b^2\rangle}{N_{cb}a^2}\right\} \tag{38}$$

where A_{int} is the interfacial area being considered, Q is the number of block copolymer chains in the interfacial film, and $\langle R_a^2\rangle$ and $\langle R_b^2\rangle$ are the mean-squared end-to-end distances of the A and B copolymer blocks, respectively. The following relations are obtained from the assumption that $\langle R_a^2\rangle^{1/2} + \langle R_b^2\rangle^{1/2} = z_i^*$:

$$\langle R_a^2\rangle = \left(\frac{QN_{ca}}{\rho_0 A_{int}}\right)^2, \quad \langle R_b^2\rangle = \left(\frac{QN_{cb}}{\rho_0 A_{int}}\right)^2 \tag{39}$$

The interfacial layer is treated as a separate phase, which must be in equilibrium with the bulk phases. The chemical potential of block copolymer is given by $\mu_c = (\delta F/\delta Q)_{A_{int}}$ whereas the interfacial tension is given by $\gamma = (\delta F/\delta A_{int})_Q$, and one obtains the expressions for these two quantities

$$\frac{\mu_c}{k_BT} = \frac{9\nu_i^2 N_c}{2\rho_0^2 a^2} \tag{40}$$

$$\gamma = \gamma_{ca\text{-}cb} + \gamma_{ca\text{-}ha} + \gamma_{cb\text{-}hb} - \frac{3\nu_i^3 N_c k_BT}{\rho_0^2 a^2} \tag{41}$$

where we have used $\nu_i = Q/A_{int}$. In terms of the copolymer chemical potential one obtains

$$\nu_i = \frac{\rho_0 a}{3}\left(\frac{2\mu_c}{k_BTN_c}\right)^{1/2} \tag{42}$$

$$\gamma = \gamma_{ca\text{-}cb} + \gamma_{ca\text{-}ha} + \gamma_{cb\text{-}hb} - k_BT\frac{\rho_0 a}{9}N_c^{-1/2}\left(\frac{2\mu_c}{k_BT}\right)^{3/2} \tag{43}$$

The sole negative contribution to γ, and therefore to $\Delta w(x)$, is from the fourth term in eq 43, which arises from the reduced stretching of the copolymer chains as they spread over a larger interfacial area. The sharply peaked region at the center of the $\Delta w(x)$ profile shown in Figure 10 corresponds to $\gamma_{ca\text{-}cb}$. The interface between the A and B copolymer blocks is similar to an interface between A and B homopolymers of molecular weights N_{ca} and N_{cb}, with the added requirement that the copolymer joints lie within an interfacial region of width d. The following approximate expression for $\gamma_{ca\text{-}cb}$ is obtained by taking into account the entropy loss associated with the confinement of the copolymer joints to this interfacial region:

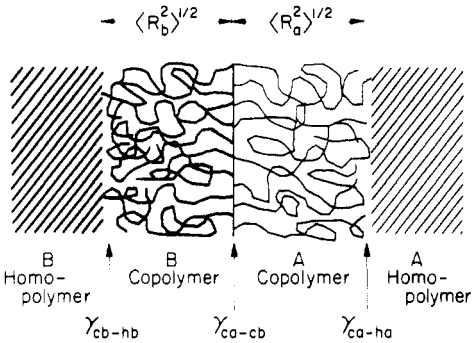

Figure 11. Schematic diagram of a segregated copolymer layer, showing the three different interfaces that are formed at high values of the copolymer chemical potential.

$$\gamma_{ca\text{-}cb} = \gamma_0(N_{ca},N_{cb}) + \nu_i k_BT \ln\{(z_i^*)/d\} \tag{44}$$

The positive contributions to $\Delta w(x)$, which appear at the outer edges of the segregated layer as shown in Figure 10, correspond to $\gamma_{ca\text{-}ha}$ and $\gamma_{cb\text{-}hb}$. As demonstrated by the profiles in Figure 2, the interfaces between the copolymer and the homopolymers are relatively broad. Estimates of $\gamma_{ca\text{-}ha}$ and $\gamma_{cb\text{-}hb}$ are obtained by integrating the form of $k(x)$, which is valid for broad interfaces:

$$\gamma_{ca\text{-}ha} + \gamma_{cb\text{-}hb} = \rho_0 k_BT \int_{-\infty}^{+\infty} \frac{a^2}{36\phi_c(x)(1-\phi_c(x))} \times \left(\frac{\partial\phi_c(x)}{\partial x}\right)^2 dx \tag{45}$$

Equations 44 and 45 for the interfacial terms are complicated, but an approximate analytic expression for the interfacial tension can be obtained by assuming that $\gamma_{ca\text{-}cb} + \gamma_{ca\text{-}ha} + \gamma_{cb\text{-}hb} = \gamma_0^\infty$. This approximation is implicit in the derivation described by Leibler in ref 6. Predictions for γ and ν_i from this approximate theory are shown in Figure 12 for a 200–200 copolymer with $\chi_{ab} = 0.1$ and $N_h = 1000$. Values obtained from the solution of the complete set of mean-field equations are also included. The numerically calculated values of ν_i approach the values from the simplified theory at the highest values of μ_c. The assumption that only the stretching free energy contributes to the chemical potential of the interfacial layer is therefore reasonable in the limit of high μ_c. This stretching free energy is independent of χ_{ab} and is determined primarily by the degree of polymerization of the longer copolymer block. The way in which the interfacial density of copolymer chains varies with the molecular parameters for high μ_c as mentioned in the previous section is consistent with this result.

Figure 12 also indicates that γ_0^∞ is not a good approximation to the interfacial terms for high values of the copolymer chemical potential. The different contributions to γ as obtained from eqs 44 and 45 for a 200–200

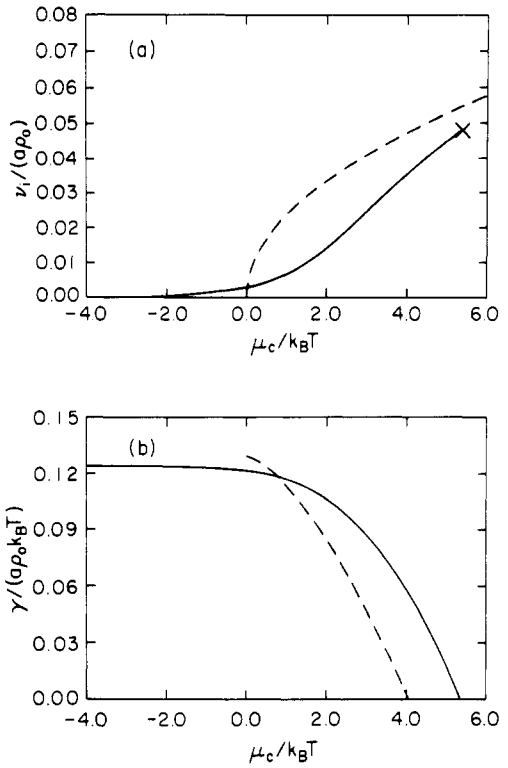

Figure 12. Interfacial parameters as a function of μ_c for $N_{ca} = N_{cb} = 200$, $N_{ha} = N_{hb} = 1000$, and $\chi_{ab} = 0.1$, showing values calculated from the complete solution to the mean-field equations (—) and values from the scaling theory as described in ref 6 (- - -): (a) normalized interfacial density of copolymer chains, (b) normalized interfacial tension.

Table III
Contributions to the Interfacial Tension for a 200–200 Copolymer with $\mu_c = 4k_BT$, $N_h = 1000$, and $\chi_{ab} = 0.1$

$\gamma_0(N_{ca}, N_{cb})$	$0.111a\rho_0k_BT$
localization of joints	$0.052a\rho_0k_BT$
$\gamma_{ca\text{-}ha} + \gamma_{cb\text{-}hb}$	$0.014a\rho_0k_BT$
chain stretching	$-0.126a\rho_0k_BT$
total	$0.051a\rho_0k_BT$
actual calculated γ	$0.057a\rho_0k_BT$

copolymer with $N_h = 1000$, $\mu_{ca} = 4k_BT$, and $\chi_{ab} = 0.1$ are listed in Table III. We have used the profiles shown in Figure 2 in order to estimate $\gamma_{ca\text{-}ha} + \gamma_{cb\text{-}hb}$ from eq 45. A significant contribution to the interfacial tension is associated with the localization of the copolymer joints to the central interfacial region of width d. The decrease in $\Delta\gamma$ with increasing χ_{ab} as shown in Figure 6 arises from the increased localization of copolymer joints for higher values of χ_{ab}.

The data in Table III suggest that the free energy associated with the interfaces between the copolymer layer and the homopolymers is relatively small. This interfacial free energy is still important in that it can give rise to an attractive interaction between adsorbed polymer layers. Consider for example the adsorption of an A/B diblock copolymer from solution onto surfaces that have a preferential attraction for the B block, as shown schematically in Figure 13. In our case the surfaces represent A/B homopolymer interfaces and the solvent is A homopolymer, but the argument that follows is valid in general for end-adsorbed polymer layers. We assume that the free energy of the individual segregated layers is independent of their separation. Interactions between the layers are therefore determined by $\gamma_{ca\text{-}ha}$ and $\gamma_{ca\text{-}ca}$, where $\gamma_{ca\text{-}ha}$ is as defined above and $\gamma_{ca\text{-}ca}$ is the interfacial tension between two segregated layers. An osmotic term associated

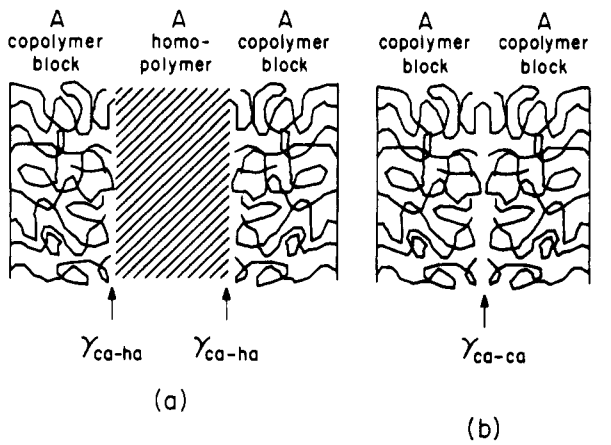

Figure 13. Schematic diagram of two adsorbed copolymer layers that illustrate the origin of the attractive interaction: (a) separated adsorbed layers, (b) adsorbed layers in contact with one another.

with the exclusion of homopolymer from between the segregated layers gives a positive contribution to $\gamma_{ca\text{-}ca}$, which is inversely proportional to the homopolymer degree of polymerization. For a very high homopolymer degree of polymerization this osmotic term will be negligible and one expects that $\gamma_{ca\text{-}ca}$ will be approximately equal to $\gamma_{ca\text{-}ha}$. The overall interfacial free energy of the system can therefore be decreased by an amount equal to $\gamma_{ca\text{-}ha}$ by bringing the two separated copolymer layers into contact with each other. The segregation of block copolymer micelles to interfaces as described in ref 5 is a manifestation of this type of attractive interaction.

Finally, we point out that the simple scaling treatment and the mean-field treatment described here are completely compatible, as is necessary for the validity of the previous discussion. The underlying assumption in both cases is that the polymer chain conformations are only mildly distorted from their ideal random-walk conformations. Equations such as eq 38, with terms of the form R^2/na^2, are valid only in this limit. The copolymer blocks are in fact stretched away from the interface, but over distances that are a small fraction of the overall contour lengths of these blocks. The advantage of the complete mean-field treatment described here is that additional simplifying assumptions are not necessary.

Conclusions

The complete set of mean-field equations describing the interface between homopolymer phases in the presence of block copolymers can be solved numerically. The results give quantitative predictions for the interfacial profiles and the interfacial tension, which would avoid approximations typically associated with analytic treatments. Here we list some general results from our calculations.

1. An increase in the copolymer chemical potential is accompanied by an increase in the density of block copolymer chains at the interface and by a decrease in the interfacial tension. A theoretical determination of the limiting value of the copolymer chemical potential associated with the formation of block copolymer micelles must be obtained separately.

2. The maximum copolymer volume fraction in the interfacial region can be quite close to one, even for intermediate values of the copolymer chemical potential, which correspond to a significant interfacial tension.

3. The confinement of copolymer joints to the central portion of the interfacial region contributes significantly to the interfacial tension and gives rise to a broadening of the A–B segmental profile. The specific width of this

segmental profile is determined largely by the strength of the unfavorable interaction between A and B segments.

4. For high values of the copolymer chemical potential, the total copolymer segregation and the overall copolymer concentration profile are determined primarily by the free energy associated with the extension of the copolymer blocks away from the interface. The overall copolymer concentration profile therefore does not depend strongly on the details of the thermodynamic interaction between A and B segments.

5. The free energy associated with the interface between a segregated polymer layer and a high molecular weight homopolymer matrix can give rise to an attractive interaction between segregated layers.

Acknowledgment. This work was supported by the NSF-DMR Materials Program through the Cornell Materials Science Center. K.R.S. was funded by AT&T in the form of a Ph.D. fellowship. We have also benefited from helpful discussions with Richard Jones, and we thank Daniel Broseta for supplying a preprint of ref 26.

Appendix: Method of Solution

Here we outline the iterative procedure for solving the mean-field equations in a self-consistent manner. The interface position is at $x = 0$, with the A-rich phase existing at positive values of x and the B-rich phase existing at negative values of x. The mean fields are expressed as the sum of two terms:

$$w_a(x) = w_a^\circ(x) - w'(x) \quad \text{(A-1)}$$

$$w_b(x) = w_b^\circ(x) - w'(x) \quad \text{(A-2)}$$

The difference between w_a and w_b is entirely in the components w_a° and w_b°

$$w_a^\circ(x) = \chi_{ab}\phi_b^2(x) \quad \text{(A-3)}$$

$$w_b^\circ(x) = \chi_{ab}\phi_a^2(x) \quad \text{(A-4)}$$

whereas w' is identical for A and B segments and includes $K_\phi(x)$:

$$w'(x) = \Delta w_{eff}(x) + K_\phi^{bulk} \quad \text{(A-5)}$$

Here $K_\phi(x)$ is given by

$$K_\phi(x) = \frac{\phi_{ha}(x)}{N_{ha}} + \frac{\phi_{hb}(x)}{N_{hb}} + \frac{\phi_{ca}(x) + \phi_{cb}(x)}{N_{ca} + N_{cb}} \quad \text{(A-6)}$$

and K_ϕ^{bulk} is the value of K_ϕ in the bulk phase on the appropriate side of a dividing surface at $x = 0$. The difference $K_\phi(x) - K_\phi^{bulk}$ is accounted for in the undetermined function $\Delta w_{eff}(x)$.

We begin with assumed concentration profiles for the components, which interpolate between the correct bulk phase values. From these profiles we calculate mean fields for the A and B segments, with $\Delta w_{eff}(x) = 0$ initially. The modified diffusion equations for the six distribution functions are then solved numerically via the Crank–Nicholson scheme as described by Hong and Noolandi.[16] The equations for q_{ha}, q_{ca}, q_{hb}, and q_{cb} are solved first.

$$\frac{1}{N_{ha}}\frac{\partial q_{ha}(x,t)}{\partial t} = \frac{a^2}{6}\frac{\partial^2 q_{ha}(x,t)}{\partial x^2} - \frac{w_a(x)}{k_B T} q_{ha}(x,t) \quad \text{(A-7)}$$

with the initial condition $q_{ha}(x,0) = 1$ and the boundary conditions $q_{ha}(\infty,t) = \exp(-N_{ha}t w_a(\infty)/k_B T)$ and $q_{ha}(-\infty,t) = \exp(-N_{ha}t w_a(-\infty)/k_B T)$.

$$\frac{1}{N_{ca}}\frac{\partial q_{ca}(x,t)}{\partial t} = \frac{a^2}{6}\frac{\partial^2 q_{ca}(x,t)}{\partial x^2} - \frac{w_a(x)}{k_B T} q_{ca}(x,t) \quad \text{(A-8)}$$

with the initial condition $q_{ca}(x,0) = 1$ and the boundary conditions $q_{ca}(\infty,t) = \exp(-N_{ca}t w_a(\infty)/k_B T)$ and $q_{ca}(-\infty,t) = \exp(-N_{ca}t w_a(-\infty)/k_B T)$.

$$\frac{1}{N_{hb}}\frac{\partial q_{hb}(x,t)}{\partial t} = \frac{a^2}{6}\frac{\partial^2 q_{hb}(x,t)}{\partial x^2} - \frac{w_b(x)}{k_B T} q_{hb}(x,t) \quad \text{(A-9)}$$

with the initial condition $q_{hb}(x,0) = 1$ and the boundary conditions $q_{hb}(\infty,t) = \exp(-N_{hb}t w_b(\infty)/k_B T)$ and $q_{hb}(-\infty,t) = \exp(-N_{hb}t w_b(-\infty)/k_B T)$.

$$\frac{1}{N_{cb}}\frac{\partial q_{cb}(x,t)}{\partial t} = \frac{a^2}{6}\frac{\partial^2 q_{cb}(x,t)}{\partial x^2} - \frac{w_b(x)}{k_B T} q_{cb}(x,t) \quad \text{(A-10)}$$

with the initial condition $q_{cb}(x,0) = 1$ and the boundary conditions $q_{cb}(\infty,t) = \exp(-N_{cb}t w_b(\infty)/k_B T)$ and $q_{cb}(-\infty,t) = \exp(-N_{cb}t w_b(-\infty)/k_B T)$. In cases where the bulk phases are essentially pure homopolymer A and pure homopolymer B, the boundary conditions are simplified by the fact that $w_a(-\infty)/k_B T = w_b(\infty)/k_B T = \chi_{ab}$ and $w_a(\infty) = w_b(-\infty) = 0$.

At this point we are in a position to solve the equations for q_{ab} and q_{ba}

$$\frac{1}{N_{ca}}\frac{\partial q_{ab}(x,t)}{\partial t} = \frac{a^2}{6}\frac{\partial^2 q_{ab}(x,t)}{\partial x^2} - \frac{w_a(x)}{k_B T} q_{ab}(x,t) \quad \text{(A-11)}$$

with the initial condition $q_{ab}(x,0) = q_{cb}(x,1)$ and the boundary conditions $q_{ab}(\infty,t) = \exp(-N_{ca}t w_a(\infty)/k_B T - N_{cb}w_b(\infty)/k_B T)$ and $q_{ab}(-\infty,t) = \exp(-N_{ca}t w_a(-\infty)/k_B T - N_{cb}w_b(-\infty)/k_B T)$.

$$\frac{1}{N_{cb}}\frac{\partial q_{ba}(x,t)}{\partial t} = \frac{a^2}{6}\frac{\partial^2 q_{ba}(x,t)}{\partial x^2} - \frac{w_b(x)}{k_B T} q_{ba}(x,t) \quad \text{(A-12)}$$

with the initial condition $q_{ba}(x,0) = q_{ca}(x,1)$ and the boundary conditions $q_{ba}(\infty,t) = \exp(-N_{cb}t w_b(\infty)/k_B T - N_{ca}w_a(\infty)/k_B T)$ and $q_{ba}(-\infty,t) = \exp(-N_{cb}t w_b(-\infty)/k_B T - N_{ca}w_a(-\infty)/k_B T)$.

Volume fractions of each homopolymer and of each block of the copolymer are calculated from the following equations:

$$\phi_{ha}(x) = \exp(\mu_{ha}/k_B T - 1)\int_0^1 q_{ha}(x,t)\, q_{ha}(x,1-t)\, dt \quad \text{(A-13)}$$

$$\phi_{hb}(x) = \exp(\mu_{hb}/k_B T - 1)\int_0^1 q_{hb}(x,t) q_{hb}(x,1-t)\, dt \quad \text{(A-14)}$$

$$\phi_{ca}(x) = \frac{N_{ca}}{N_c}\exp(\mu_{ca}/k_B T - 1)\int_0^1 q_{ca}(x,t)\, q_{ab}(x,1-t)\, dt \quad \text{(A-15)}$$

$$\phi_{cb}(x) = \frac{N_{cb}}{N_c}\exp(\mu_c/k_B T - 1)\int_0^1 q_{cb}(x,t)\, q_{ba}(x,1-t)\, dt \quad \text{(A-16)}$$

These volume fractions and eqs A-3–A-5 are used to calculate the "image" mean-field components $w_{aI}^\circ(x)$, $w_{bI}^\circ(x)$, and $w_I'(x)$, which correspond to the original, assumed mean fields. The quantity $w_{eff}(x)$ is given by

$$\Delta w_{eff} = \zeta\{1 - \phi_{ha}(x) - \phi_{hb}(x) - \phi_{ca}(x) - \phi_{cb}(x)\} \quad \text{(A-17)}$$

New mean-field components, w_{aN}°, w_{bN}°, and w_N', are derived from a combination of the original guesses and the

image mean fields as follows:

$$w_{aN}^{\circ}(x) = (1 - \lambda_1)w_a^{\circ}(x) + \lambda_1 w_{aI}^{\circ}(x) \quad \text{(A-18)}$$

$$w_{bN}^{\circ}(x) = (1 - \lambda_1)w_b^{\circ}(x) + \lambda_1 w_{bI}^{\circ}(x) \quad \text{(A-19)}$$

$$w_N'(x) = (1 - \lambda_2)w'(x) + \lambda_2 w_I'(x) \quad \text{(A-20)}$$

where λ_1 and λ_2 are constants. Mean-field guesses for the next iteration are constructed from w_{aN}°, w_{bN}°, and w_N' according to eqs A-1 and A-2, and the entire process is repeated until the following convergence conditions are satisfied for all values of x

$$|w_a^{\circ}(x) - w_{aI}^{\circ}(x)|, |w_b^{\circ}(x) - w_{bI}^{\circ}(x)| < \epsilon_1 \quad \text{(A-21)}$$

$$|\sum_k \phi_k(x) - 1| < \epsilon_2 \quad \text{(A-22)}$$

where we typically use $\epsilon_1 = 10^{-4}$ and $\epsilon_2 = 10^{-3}$. Appropriate values of λ_1 and λ_2 must be chosen so that the solution converges. Empirically we find that $\chi_{ab}\lambda_1 N$ and $\zeta\lambda_2 N$ must be less than approximately 2 for stability, where N is the degree of polymerization of the largest molecule in the system. The incompressibility parameter, ζ, must be chosen such that the solution will ultimately converge to a state that satisfies eq A-22. We typically use $\zeta = 100\chi_{ab}$. The interfacial tension is given by

$$\gamma = \rho_0 \int_{-\infty}^{+\infty} \{w'(x) - K_\varphi(x)\}\, dx \quad \text{(A-23)}$$

References and Notes

(1) Gaillard, P.; Ossenbach-Sauter, M.; Reiss, G. *Makromol. Chem., Rapid Commun.* **1980**, *1*, 771.
(2) Anastasiadis, S. H.; Gancarz, I.; Koberstein, J. T. *Macromolecules* **1989**, *22*, 1449.
(3) Brown, H. R. *Macromolecules* **1989**, *22*, 2859.
(4) Creton, C.; Hui, H. C. Y.; Kramer, E. J.; Hadziioannou, G.; Brown, H. R. *Bull. Am. Phys. Soc.* **1989**, *34*, 709.
(5) Shull, K. R.; Kramer, E. J. *Macromolecules*, following paper in this issue.
(6) Leibler, L. *Makromol. Chem., Macromol. Symp.* **1988**, *16*, 1.
(7) Helfand, E.; Tagami, Y. *Polym. Lett.* **1971**, *9*, 741.
(8) Helfand, E.; Tagami, Y. *J. Chem. Phys.* **1972**, *56*, 3592.
(9) Helfand, E.; Tagami, Y. *J. Chem. Phys.* **1972**, *57*, 1812.
(10) Helfand, E.; Sapse, A. M. *J. Chem. Phys.* **1975**, *62*, 1327.
(11) Helfand, E. *J. Chem. Phys.* **1975**, *62*, 999.
(12) Helfand, E. *Macromolecules* **1975**, *8*, 552.
(13) Helfand, E.; Wasserman, Z. R. *Macromolecules* **1976**, *9*, 879.
(14) Helfand, E.; Wasserman, Z. R. *Macromolecules* **1978**, *11*, 960.
(15) Helfand, E.; Wasserman, Z. R. *Macromolecules* **1978**, *11*, 994.
(16) Hong, K. M.; Noolandi, J. *Macromolecules* **1981**, *14*, 727.
(17) Hong, K. M.; Noolandi, J. *Macromolecules* **1981**, *14*, 736.
(18) Noolandi, J.; Hong, K. M. *Macromolecules* **1982**, *15*, 482.
(19) Noolandi, J.; Hong, K. M. *Macromolecules* **1984**, *17*, 1531.
(20) Vilgis, T. A.; Noolandi, J. *Makromol. Chem., Macromol. Symp.* **1988**, *16*, 225.
(21) Sanchez, I. C. *Encycl. Polym. Sci. Technol.* **1987**, *11*, 1.
(22) Cahn, J. W.; Hilliard, J. E. *J. Chem. Phys.* **1958**, *28*, 1958.
(23) Edwards, S. F. *Proc. Phys. Soc. London* **1965**, *85*, 613.
(24) Leibler, L.; Orland, H.; Wheeler, J. C. *J. Chem. Phys.* **1983**, *79*, 3550.
(25) Wang, Z.-G.; Safran, S. A. *J. Phys.* **1990**, *51*, 185.
(26) Broseta, D.; Fredrickson, G. H.; Leibler, L. *Macromolecules* **1990**, *23*, 132.
(27) Noolandi, J.; Hong, K. M. *Macromolecules* **1983**, *16*, 1443.